Quantum Turbulence, and How it is Related to Classical Turbulence

Xueying Wang
xueying8@illinois.edu
University of Illinois at Urbana-Champaign

May 13, 2018

Abstract

Since the discovery of turbulence in superfluid, great attention has been paid in finding out and understanding its properties. One way to understand quantum turbulence is by comparing it to classical turbulence. In recent researches, some similarities and differences between the properties of quantum turbulence and classical turbulence have been found. In this essay, analytical models, experimental and numerical results on turbulence in He II will be discussed and compared to the properties of classical turbulence. I will focus on the similarity and difference in energy spectrum of He II turbulence and classical turbulence. The cause of the similarity and difference will also be addressed briefly. Finally, ongoing research problems concerning quantum turbulence and its relationship with classical turbulence will be briefly discussed at the end of this essay.

This is the term essay for Phys 569: Emergent State of Matter taught by Professor Nigel Goldenfeld.

1 Introduction

1.1 Focus of this Essay

Classical turbulence (CT) is the turbulence of classical fluid characterized by the chaotic motion of its flow. It is the last classical physics problem that is not solved. Quantum turbulence (QT), on the other hand, is characterized by the tangle of quantum vortices, the defects in quantum fluid.

Since the discovery of QT, many attentions have been drawn into it. At first, researchers did not realize the similarity of QT and CT, and research on QT followed methods independent of that in CT for a long time. It was after the discovery of co-flow turbulence in He II that researchers started to compare QT with CT, which largely helped in the understanding of QT. Recently, as QT has been better understood, it is actually starting to provide insights in the comprehension of CT.

QT has been studied in systems like ^4He,^3He, and atomic Bose-Einstein condensate. In this term essay, I will discuss QT in ^4He, with a focus on its energy spectrums, and try to interpret the origin of the similarity and difference between the energy spectrum of QT and CT.

1.2 Why Interested in the Problem?

CT is a completely classical problem, while QT is caused by the tangle of vortices, which is the discrete excitations appearing in the Bose-Einstein condensate ground state (superfluid state), and so it is caused by quantum effect.

It is curious that such two seemingly different systems should share common properties, which makes it interesting to find out the cause of such similarity. And it is also interesting to know where such similarity would lead us, and where it would end.

Besides similarity itself, it is also exciting to know that recent works in QT have been contributing to our understanding of CT! Since the vortex structure of quantum fluid is simpler than that in CT, it is possible that we are able to make use of the similarity between QT and CT to understand the behavior of CT. So, studies on QT may lead to a breakthrough in the unsolved CT problems that has long been puzzling us.

2 Theoretical Backgrounds

2.1 Properties of Classical Turbulence

CT has been studied long before the discovery of QT, and some of its properties have been confirmed and accepted as basic features of turbulence. When researchers started looking at the similarity between QT and CT, seeking the properties of CT in QT naturally became their guideline of research. So, in order to compare CT and QT, we need to first introduce some properties of CT.

2.1.1 The Richardson Cascade and Kolmogorov Hypothesis

Because of the dissipation in the system, to keep a turbulent fluid system steady (not decaying), one need to continuously input energy to the system. The idea of energy cascade in turbulence was purposed by Richardson, and that is why it is often known as *the Richardson cascade*. The idea of Richardson cascade is that the injection of energy happens at large scale, scale of the energy containing eddies $l_e \sim L, the\ length\ scale\ of\ the\ system$, and the dissipation happens in small scale η, the Kolmogorov length scale. Typically, in 3D, the injected energy is transported from large scale to small scale by breaking large eddies into small ones, and small eddies into smaller ones.

Kolmogorov further developed the idea of energy cascade by purposing his hypothesis on turbulence and dividing the system into three regions according to the length scale. Here is his hypothesis:

- When the Reynolds number Re of the system is very high, the system would be in equilibrium state (in which at each moment, the energy input equals to the dissipated energy), where the system can be uniquely determined by energy dissipation rate ϵ and kinematic viscosity ν, and when the state is reached, the turbulence is statistically homogeneous and locally isotropic.
- When this above-mentioned equilibrium state is reached, there exists a length scale l satisfying $\eta << l << l_e$, where the dissipation only depends on ϵ, but not on ν. The corresponding range in $k - space$ with wave vector k satisfying $\frac{2\pi}{l_e} << k << \frac{2\pi}{\eta}$ is called the inertial range.

From these hypotheses, we can get the energy spectrum of the turbulence system in the inertial range by dimensional analysis:

$$E(k) = C\epsilon^{2/3}k^{-5/3} \tag{1}$$

This is the famous Kolmogorov spectrum, and it has been generally confirmed by experiments in CT.

We can also determine the Kolmogorov length scale by dimensional analysis:

$$\eta = (\nu/\epsilon)^{1/4} \tag{2}$$

Besides inertial range, the other two ranges are called $injective\ range(k \sim \frac{2\pi}{L})$ and $dissipative\ range(k \sim \frac{2\pi}{\eta})$.

2.1.2 Vortex Structure in CT

In CT, vortex is a region where fluid revolves around an axis line. We can define vorticity $\vec{\omega}$ to be $\nabla \times \vec{u}$, where $\vec{u}$ is the local velocity of the fluid.

Vortices are generated in classical fluid because of the inherent instability of the system. In CT, vortices are instable. Their structures can change over time, and the value that vorticity $\vec{\omega}$ can take is arbitrary (not quantized).

The interaction of classical vortices in CT is still an ongoing research topic, and the role of vortex reconnection in CT is still not fully understood.

2.2 Quantum Fluid and Its Different Levels of Descriptions

2.2.1 Topological Defects and Vortices in QT

As was discussed in the course[2], in the superfluid phase of ^4He (He II phase), the system goes through Bose-Einstein Condensate and the ground state (the superfluid component) can be described with a single wave function $\psi = \psi_0 e^{i\theta}$, and the velocity of the superfluid is given by $\vec{v} = \frac{\hbar}{m}\nabla\theta$. So, for single connected area of superfluid, the velocity field would be curl-less $\nabla \times \vec{v} = 0$. Around topological defect (the discrete points in space where ψ vanishes), $\oint_c \vec{v} \cdot d\vec{l} = \int_s \nabla \times \vec{v}\ d\vec{S} = \frac{2\pi\hbar n}{m}$, $(n \in Z)$ has to be quantized. In 3D, these topological defects are line-like objects and they are the so-called quantum vortices.

Quantum vortex differs from classical vortex, in that they are quantized and they are line-like objects in 3D, so their structures and vorticities are definite. As a result, structure of quantum vortex is much simpler than its classical counterpart.

2.2.2 A Coarse-Grained Microscopic Description: Gross-Pitaevskii Equation

Also as shown in the course[2], we can derive the Gross-Pitaevskii Equation, the equation of motion of the condensate wave function by directly computing from the Heisenberg equation of motion with the Bogoliubov Hamiltonian in real space, and we end up with:

$$(i\hbar\frac{\partial}{\partial t} + \frac{\hbar^2}{2m}\nabla^2)\psi = U_0\psi|\psi|^2 \tag{3}$$

, where $U_0 = \frac{4\pi\hbar^2 a}{m}$($a$ is the s-wave scattering length in Born approximation) is the amplitude of the pseudo-potential. This equation is also known as the Nonlinear Schrodinger Equation. It can be used to describe the behavior of He II when the excitations can be neglected, in other words, when $T \to 0$. The G-P Model can describe the reconnection and nucleation that is concerned with the vortex core.

By Madelung transformation $\psi = \sqrt{\rho}e^{i\theta}$, Gross-Pitaevskii equation can be transformed into the form of Euler equation:

$$\partial_t\rho + \partial_j(\rho v_j) = 0 \tag{4}$$

$$\rho\partial_t v_j + \rho v_k\partial_k v_j = -\partial_j p + \partial_k S_{jk} \tag{5}$$

, where $p = 1/2\rho$, $S_{jk} = \frac{\varrho}{4}\partial^2_{jk} ln\rho$. The last term in Eqn.5 comes from quantum effect, without which the equations are the dynamical equations for the Euler fluid.

2.2.3 A Macroscopic Description: Vortex Filament Model

Vortex filament model describes the motion of existing vortices in the system. Because of the curl-less property of the superfluid velocity field $\nabla \times \vec{v} = 0$, it resembles the static magnetic

field $\nabla \times \vec{B} = 0$. As a result, the superfluid velocity field v_s around a vortex can be calculated with the Biot-Savart law:

$$\vec{v_s}(r) = \frac{n}{4\pi}\int_l \frac{(\vec{s_1} - \vec{r}) \times d\vec{s_1}}{|\vec{s_1} - \vec{r}|^3} \tag{6}$$

, where n is quantum of circulation, and s_1 is a point on the vortex line.

Eqn. 6 is divergent on vortex core. So, for velocity of vortex filament:

$$\vec{\dot{s}} = \frac{n}{4\pi}\vec{s'} \times \vec{s''} ln(\frac{2(l_+ l_-)^{1/2}}{e^{1/4} a_0}) + \frac{n}{4\pi}\int_l \frac{(\vec{s_1} - \vec{r}) \times d\vec{s_1}}{|\vec{s_1} - \vec{r}|^3} \tag{7}$$

, where the second term is the same as in Eqn.6, representing the nonlocal contribution from the superfluid component, while the first term represents the interaction of the vortex with itself. a_0 is the radius of the vortex core, s' and s'' are the first and second order differentiate along the vortex filament.

Eqn.7 can be used to model He II when $T \to 0$. When temperature is non-zero, a phenomenological dissipation force, the mutual friction, is added to the equation to account for the friction between the normal fluid and superfluid components. For the vortex filament model, the mutual friction is given in terms of Magnus force. The full vortex filament model at non-zero temperature is given by:

$$\vec{\dot{s}}_{full} = \vec{\dot{s}} + \alpha \vec{s'} \times (\vec{v}_n - \vec{\dot{s}}_0) - \alpha' \vec{s'} \times (\vec{s'} \times (\vec{v}_n - \vec{\dot{s}}_0)) \tag{8}$$

A simplified version of the vortex filament model is called the localized induction approximation (LIA) model, given by,

$$\vec{\dot{s}} = \frac{n}{4\pi} ln(\frac{2(l_+ l_-)^{1/2}}{e^{1/4} a_0}) \vec{s'} \times \vec{s''} \tag{9}$$

, which ignores the nonlocal term in Eqn.7.

It is worth noticing that the vortex filament model describes how vortices that already exist evolve with time. It does not have events like vortex reconnection built in the model. As a result, the vortex reconnection has to be put in the model "by hand". For example, when numerically simulating the model, the reconnection is assumed to happen when the distance between two vortices is smaller than a threshold value.

3 The similarities between QT and CT

3.1 Experimental works

When QT was first discovered, experimental researches focused on thermal counter flow turbulence that does not have obvious classical counterpart, so it was hard to compare it to CT. However, in 1990s, it was shown that in certain turbulent system, QT satisfies the Kolmogorov spectrum in its inertial range. Here, lets look at two such experiments.

3.1.1 The grid turbulence experiment

In the grid turbulence experiment[5], researchers pulled a grid through He II, which creates a homogeneous isotropic decaying turbulence behind the grid. The behavior of vortices in He II was detected by second-sound transducers.

Although the Kolmogorov spectrum that is only valid in steady state turbulence cannot be directly compared with the situation here, the authors found a way to indirectly confirm that the Kolmogorov spectrum should be satisfied by the system if it were in a steady state turbulence instead of a decaying one.

From analysis of experimental data, they obtained the mean-square vorticity:

$$\omega^2 \sim -\frac{1}{\nu}\frac{\partial u'^2}{\partial t} \tag{10}$$

, (where u' is the mean-square velocity fluctuation, and ν is the kinematic viscosity). Applying Kolmogorov's idea that energy is injected at length scale l_e, and dissipated at length scale η, they got the energy dissipation rate by dimensional analysis:

$$\epsilon = \epsilon_0 u'^3 / l_e \tag{11}$$

,where ϵ_0 is a dimensionless constant. They assumed that analysis on classical grid turbulence applies here, and assumed l_e is a constant equal to the system size. And from the above two relations, they got:

$$\omega \sim (\frac{2}{\nu})^{1/2}\frac{3l_e}{\epsilon_0}t^{-3/2} \tag{12}$$

The experimental results confirmed this power law relationship between ω and $t^{-3/2}$, as is shown in Fig.1, where the left panel shows a typical $\omega - t$ data. And on the left panel, m is the exponent of $\omega \sim t^{-m}$ fitted from the data, which should take the value of 1.5 according to Eqn.12, which is shown by the dashed line. So from the right panel of Fig.1, it is shown that for systems with different Reynolds number, the values of m all fluctuate around the theoretical value $m = 1.5$. In this way, they indirectly proved that the system satisfies the Kolmogorov spectrum.

3.1.2 The Counter-Rotating Disk Experiment

Another experiment that shows the Kolmogorov power law behavior in QT[6] was conducted by generating turbulence in He II between two counter-rotating disks, and the energy spectrum was detected by measuring the pressure fluctuation.

In this case, since the system is in steady state turbulence, the energy spectrum can be directly compared to Kolmogorov spectrum. As is shown in Fig.2, for ^4He at different temperature both above and below λ-point (about $2.17K$ @ $1\ atm.$), E scales as $E \propto f^{-5/3}$. With the Taylor frozen Hypothesis (long time observation of the flow pasting a fixed point is assumed to be the same as observation of the flow at different points in space), the scaling can be mapped onto $E \propto k^{-5/3}$, which means that Kolmogorov power law is satisfied. Also, since

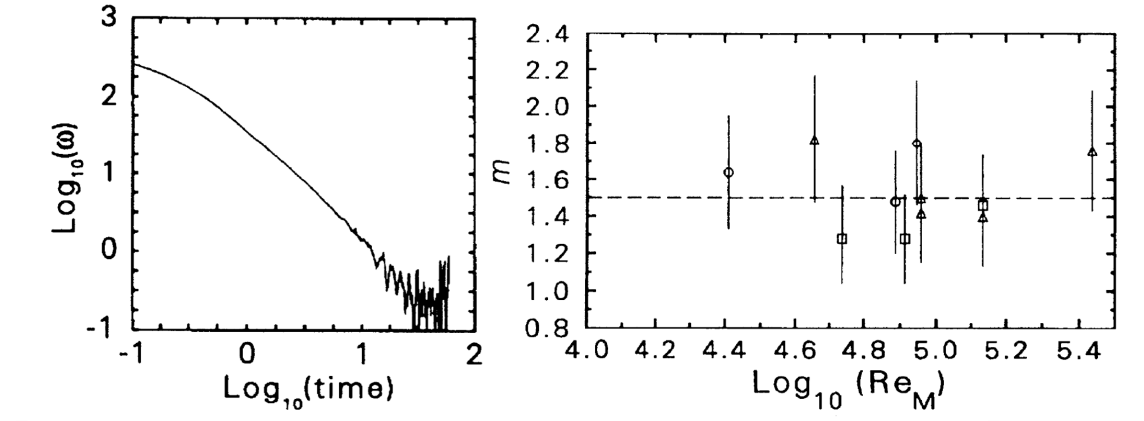

Figure 1: Power law dependence of ω and t from[5], left panel shows the experimental results of $omega - t$, right panel shows the result of m fitted from $\omega \sim t^{-m}$. Theoretical value is given by the dashed horizontal line

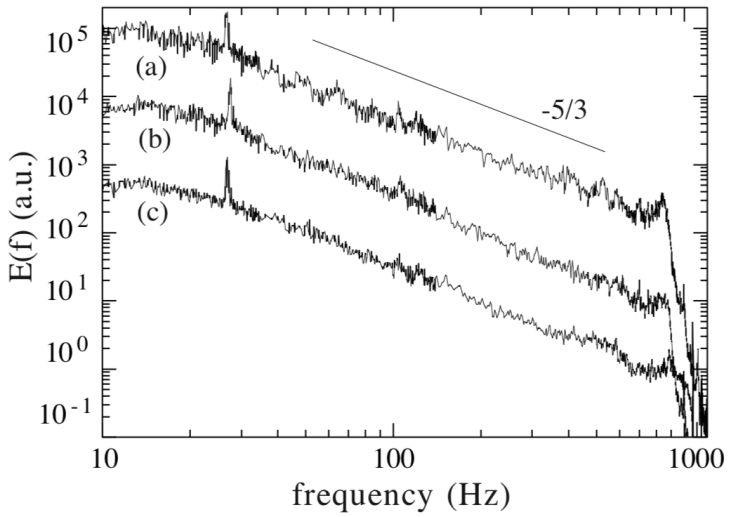

Figure 2: Energy spectrum measured in the counter-rotating disk experiment from[6] (a)T=2.3K (b)T=2.08K (c)T=1.4K

below the λ-point, the ratio of superfluid component ρ_s/ρ is a function of temperature, the fact that the same $f^{-5/3}$ scaling is satisfied for both $T = 2.08K$ and $T = 1.4K$ shows that the Kolmogorov spectrum is satisfied despite of the different ρ_s/ρ ratio. This is a surprising result, and it was understood by interpreting the normal fluid and superfluid component to be combined by mutual friction and behave like a single fluid component.

3.2 Numerical Works

Because of the difficulty in the direct experimentally detection vortex behavior and the complexity of the analytical models, numerical studies have formed a very important part in the study of QT. I will introduce the simulation result of the two analytical models discussed in section. 2.2.2 and 2.2.3

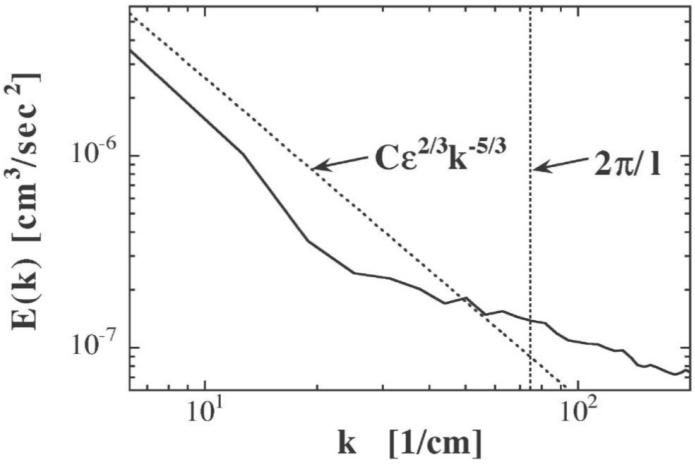

Figure 3: Kolmogorov spectrum from vortex filament simulation, from Ref.[3]

The energy spectrum of QT in He II near zero temperature was calculated using the vortex filament model with the Biot-Savart law (Eqn.6 and Eqn.7) without mutual friction[3]. They calculated a decaying turbulence, and took the result of a time-slice when homogeneous and isotropic state is reached to calculate the instant energy spectrum of the system. The way they introduce dissipation in their model is by putting vortex reconnection in the system, and by removing the vortices whose cores are of the size of the numerical resolution. The energy spectrum at T=70s when the system reached homogeneous and isotropic state is shown by the solid line in Fig.3. It is clearly shown that in the inertial range, the Kolmogorov spectrum (the dotted line) is satisfied.

The Kolmogorov spectrum is also achieved in the simulation of G-P equation (Eqn. 3). The G-P equation describes the dynamics of the condensate involving different process with different energy. Plugging $\psi(\vec{x},t) = \psi_0(\vec{x},t)e^{i\theta}$ into Eqn.3 , we can calculate the total energy of the system (setting $\hbar = 1, m = 1$):

$$E(t) = \frac{1}{N}\int d\vec{x}\ \psi^*(\vec{x},t)(-\nabla^2 + \frac{U_0}{2}\psi_0(\vec{x},t)^2)\psi(\vec{x},t) \tag{13}$$

The total energy can be separated into interaction energy $E_{int}(t)$, quantum energy $E_q(t)$ and kinetic energy $E_{kin}(t)$

$$E_{int}(t) = \frac{U_0}{2N}\int d\vec{x}\ \psi_0(\vec{x},t)^4 \tag{14}$$

$$E_q(t) = \frac{1}{N}\int d\vec{x}(\nabla\psi_0(\vec{x},t))^2 \tag{15}$$

$$E_{kin}(t) = \frac{1}{N}\int d\vec{x}(\psi_0(\vec{x},t)\nabla\psi(\vec{x},t))^2 \tag{16}$$

The kinetic energy is composed of the compressible part $E^c_{kin}(t)$ that corresponds to excitations, and the incompressible part $E^i_{kin}(t)$ which correspond to the kinetic energy of the superfluid.

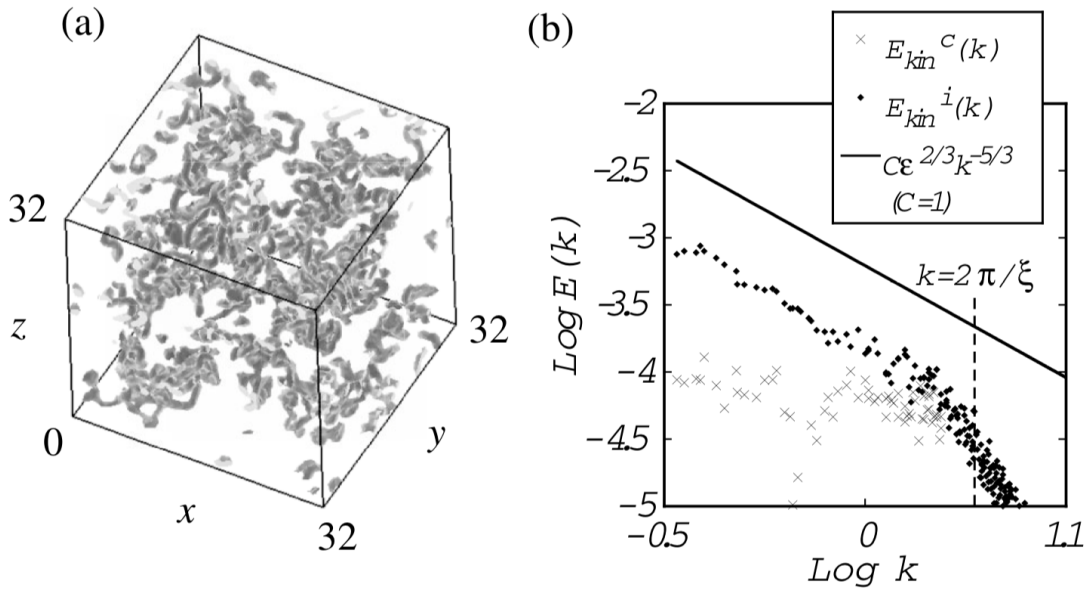

Figure 4: Kolmogorov spectrum from G-P equation simulation, from Ref.[7] (a) an instant configuration of the vortices in turbulent state (b) dot: the energy spectrum with an ensemble average over 20 runs taken; solid line: the Kolmogorov -5/3 scaling

A simulation result of a decaying turbulence in He II near $T = 0K$ using the Fourier transformed G-P Equation[7] is shown in Fig.4. The authors included a dissipation term that is only effective for scales smaller than the scale of the vortex core ξ, so as to suppress non-classical dissipation that will be discussed in section 4.1, and focus on the dissipations included in the Richardson cascade picture (section.2.1.1). In the left panel of Fig.4, an instant configuration of the system in turbulence state is shown, and on the left panel, an ensemble average over 20 runs (the dots) are compared with the Kolmogorov spectrum (the solid line). As can been seen in Fig.4, Kolmogorov spectrum is satisfied for E^i_{kin}, which represents the kinetic energy of the superfluid, in the inertial range.

3.3 Interpretation of the similarity

The reason why QT assembles CT is still not fully understood. However, there are some idea proposed by researchers that can help us fathom their similarity.

The Kolmogorov spectrum indicates a self-similarity in turbulent flow of different length scale. Although the structure of QT vortices is quite different from CT, when temperature $T \neq 0$, at length scale much larger than the scale of vortex core ξ, large scale eddies can form due to the collective behavior of bundles of vortices and resemble the behavior of eddies in CT[9].

This can happen because normal fluid eddies overlap with the vortex cores, causing the superfluid vorticity to be "comparable to the vorticity of normal fluid eddy". And when a couple of quantum vortices interact with each other, they would effectively minimize the difference in their velocity field. In this way, large eddies that resemble the behavior of classical eddies can form in superfluid component.[4].

At zero temperature where the normal fluid components can be neglected, the reason why the system still obeys the Kolmogorov spectrum can be understood from the connection between G-P equation and Euler equation shown in section 2.2.2 by Eqn.5.

A viscous incompressible fluid can be described by Navier-Stokes equation:

$$\rho[\frac{\partial u}{\partial t} + (u \cdot \nabla)u] = \nu\nabla^2 u - \nabla P \tag{17}$$

, when we nondimensionalize it with $x' := x/D, y' := y/D, z' := z/D, v := u/U, \tau := \frac{tU}{D}, p := P/P_0$, we would get:

$$\frac{\partial v}{\partial \tau} + (v \cdot \nabla')v = \frac{1}{Re}\nabla'^2 v - Eu\nabla' p \tag{18}$$

, where $Re = \frac{UD}{\mu}$ is the Reynold number, $Eu = \frac{P_0}{\rho U^2}$ is the Euler number. Comparing Eqn.5 and Eqn.17, we can see that Eqn.5 is achieved when one takes the limit of $Re \to \infty$ in Eqn. 17.

For turbulent fluid, even if the limit viscosity $\mu \to 0$ is taken, dissipation is still present in the system, the time reversal symmetry is still not recovered. This property of turbulence is referred to as *dissipation anomaly*. Because of dissipation anomaly in turbulence system, superfluid turbulence that satisfies the Euler equation Eqn.5 obeys the Kolmogorov spectrum in the inertial range.

4 Phenomenon Unique to QT

4.1 Kelvin-wave Cascade

Kelvin-wave is a deformation of vortex line that travels along the vortex line, as shown in Fig.5(a). When two vortex lines come close together, the vortex reconnection occurs, where the vortex interact with each other, they would couple their Kelvin wave modes and generate Kelvin waves with wave length that is smaller and smaller. Once the length scale of phonon emission is reached, the system would emit phonons and cause energy dissipation[9]. This process can be seen in Fig.5, as the amplitude of the Kelvin wave increases, the vortex line starts to get closer to each other and reconnection begin to happen. In Fig.5(d), you can see that the reconnection disturbs the initial configuration of the vortex lines and generate a randomly spaced vortex configuration.

The Kelvin-wave cascade is a quantum effect. It is discovered by numerical simulation and the numerical result shows that in the power spectrum in the large-k range, energy scales as $E \propto k^{-3}$.

In section 2.1.1, we discussed the energy spectrum of CT, and mentioned that the large-k region is called dissipative range. In QT however, dissipative range cannot be defined the same way, for near zero temperature, the viscosity is zero and the dissipation mechanism is no longer the same as CT. Instead, the system is governed by the Kelvin-wave cascade. A new wave vector $k_Q \simeq (\epsilon/\kappa^3)^{1/4}$ (where $\kappa = \hbar/m_{^4He}$) $l_Q = \frac{2\pi}{k_Q}$ was defined to separate the

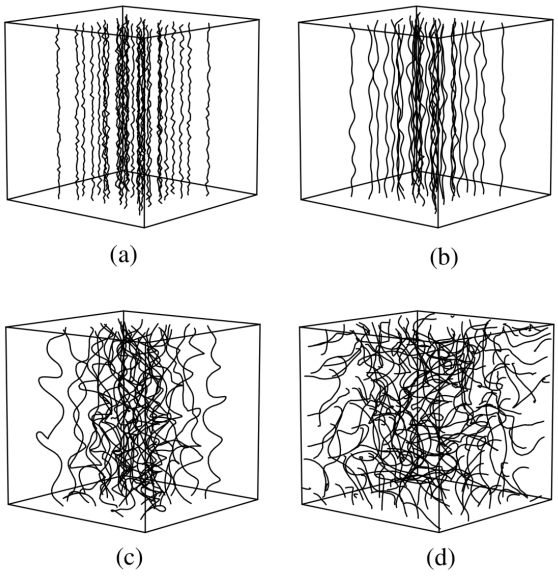

Figure 5: The numerical visualization of the Kelvin wave and reconnection between vortics, from Ref.[8] time increases from (a) to (d)

Kelvin-wave cascade range and the classical Richardson cascade range.

If the length scale l_Q is larger than the length scale l_e where the energy injection happens, then the system does not exhibit Richardson cascade, but is governed by Kelvin-wave cascade entirely. Fig.6 shows a complete energy spectrum of QT when l_Q is smaller than l_e.

4.2 Other Phenomenon Unique to QT

Since the focus of this essay is on the energy spectrum, I will only briefly mention some of the other interesting phenomenon that is unique to QT here. One of them is the counter-flow turbulence mentioned above. There is no direct classical counterpart of it, but recently, there are researchers purposing that it may be compared with convection in CT.

Another is the double transition to turbulence found in QT system. It was observed in QT system that there are two transition points when the system goes from laminar to turbulent. One phenomenological interpretation is that the two transitions correspond to the transition to turbulence of normal fluid and superfluid component separately. However, this phenomena is still not fully understood.

5 Conclusion and Discussion

5.1 Conclusion

In this term essay, semi-classical and non-classical behavior of the energy spectrum of turbulence in He II is analyzed. Experimental results of the grid turbulence experiment and the counter-rotating disk experiment at finite temperature, numerical results of the vortex filament model and G-P model at zero temperature all confirmed that Kolmogorov spectrum

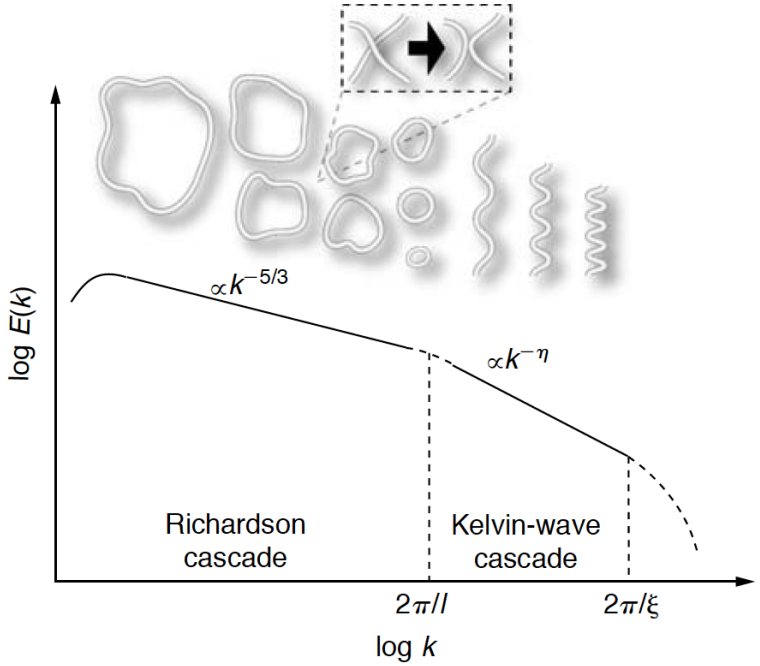

Figure 6: A complete energy spectrum of QT when l_Q is smaller than l_e, from Ref.[1]

is satisfied by He II turbulence in the inertial range. This result can be understood phenomenologically with the picture of vortices bundles forming self-similar eddies that resemble classical eddies, and the quantitatively with the connection between G-P equation and Euler equation. Furthermore, with numerical works discovering the Kelvin-wave cascade, the energy spectrum of QT is completed. Though some properties have been studied and accepted by researchers, both QT and CT are highly complicated systems with various questions to be answered. There's still a long way before we can fully figure them out.

5.2 Problems and Future Work

Properties of QT and CT is a large ongoing research topic. The view of this essay is rather limited. Here is a list of some of the problems that researchers are still working on:

- Equivalence or connection of the different models that describes quantum fluid and discovery of better models.
- Understanding CT through QT.
- What happens in the crossover region of the Richardson cascade range and Kelvin-wave cascade range? Can system transform from the classical Richardson cascade range to the quantum Kelvin-wave cascade range smoothly?
- Experimental visualization of the vortex core.
- Counter-flow turbulence in He II and whether it is related to convection in CT.

Among these problems, I would like to briefly discuss the first two here. As shown in section 2.2.3 and 2.2.2, different models have their own pros and cons. For instance, the vortex

filament model with mutual friction can be used to describe behavior of vortices at non-zero temperature, but vortex reconnection has to be artificially included, and the parameters of the mutual friction also need to be determined. With so any artificial factors, whether or not the results are reliable requires second thoughts. Recent works have been trying to resolve this issue by determining this kind of phenomenological parameters strictly. Also, simulation results of different models are compared in seek of a better model.

For the second problem, results of QT have been used to interpret CT[11][12]. However, whether this procedure works and where it will stop working depends on the fundamentals of the similarity between QT and CT. For example, when one tries to interpret CT with the vortex filament model, a question that need to be asked is whether vortex is the fundamental factor that contributes to the turbulent behavior or if it is just a 'byproduct' of turbulence.

References

[1] M. Tsubota and W. P. Halperin, Progress in Low Temperature Physics: Quantum Turbulence (Elsevier, New York, 2009)

[2] Phys 569 Emergent State of Matter Lecture Notes

[3] T. Araki, M. Tsubota, and S. K. Nemirovskii, Energy Spectrum of Superfluid Turbulence with No Normal-Fluid Component, *Phys. Rev. Lett.* 89, 145301 (2002).

[4] L. Skrbek, Quantum Turbulence, *J. Phys.* : *Conference Series* 318 (2011).

[5] M. Smith, R. Donnelly, N. D. Goldenfeld and W. F. Vinen. Decay of vorticity in homogeneous turbulence. *Phys. Rev. Lett.* 71, 2583-2586 (1993).

[6] J. Maurer and P. Tabeling, Local investigation of superfluid turbulence, *Europhysics Letters*,43, 1 (1998).

[7] M. Kobayashi and M. Tsubota, Kolmogorov Spectrum of Superfluid Turbulence: Numerical Analysis of the Gross-Pitaevskii Equation with a Small-Scale Dissipation, *Phys. Rev. Lett.* 94, 065302 (2005).

[8] M. Tsubota, T. Araki,1 and C. F. Barenghi, Rotating Superfluid Turbulence, *Phys. Rev. Lett.* 90, 20 (2003)

[9] J. Yepez, G. Vahala, L. Vahala, and M. Soe, Superfluid Turbulence from Quantum Kelvin Wave to Classical Kolmogorov Cascades, *Phys. Rev. Lett.* 103, 084501 (2009)

[10] P. R. J, Maldonado, Ph.D. Thesis, Computational Approaches to Stochastic Systems in Physics and Ecology, University of Illinois at Urbana-Champaign, 2012.

[11] L. Skrbek, and Steven R. Stalp, On the decay of homogeneous isotropic turbulence, *Phys. Fluids* 12, 1997 (2000).

[12] U. Frisch, Turbulence (Cambridge University Press, Cambridge,1995).

[13] C. F. Barenghi, L. Skrbek, and K. R. Sreenivasan, Introduction to Quantum Turbulence, *PNAS* 111(2014).